University of Rochester

Proposal

Using Metallized Silicon Nanomembranes for Modelling and Sample Processing

Author:
Karl Smith

Supervisor:
Dr. James McGrath

October 4, 2013

Specific Aims

Silicon nanomembranes (SNM) are a new technology with immediate and obvious applications in nanofiltration. SNM are made using standard (and scalable) silicon deposition and etching techniques resulting in freestanding porous membranes as thin as 15 nm [1]. Although the mean pore size of SNM is tuneable within range of 5-80 nm during the manufacturing process [2], the adjustments are empirical and based on batch processing, meaning precise control of pore distributions on a chip-by-chip basis is impractical. We propose to use oxide and metal films deposited on the surface of SNM to *control the pore size and the surface charge of the membrane*, and to exploit this modification to create a high-performance nanofluidic transistor. Nanofluidic transistors use a small gate voltage applied to a membrane to modulate how charged species migrate across the membrane in a manner analogous to the way silicon-based transistors modulate the flow of electrons. SNM are so thin relative to the size of their pores that standard molecular models of filtration do not accurately describe their behavior [3]. Using variable pore distributions and dynamically variable membrane charge, we will establish the parameters that influence sieving behavior in SNM and construct a *predictive model* for separations.

SNM are currently being studied as a possible component of human hemodialysis systems [4], lab-on-a-chip technologies [5], nanoparticle purification methods, and protein preparation [3]. The creation of both predictive models of the behavior of this novel material and methods of precisely controlling its surface charge and average pore size are a necessary and logical next step in the process of bringing this technology to fruition.

Specific Aim 1: Modulate SNM pore sieving behavior via backfilling and active control of membrane surface charge

1. Use Atomic Layer Deposition (ALD) to backfill SNM pores with Aluminum Oxide
2. Modulate the pore size distribution and porosity of SNMs using ALD and measure how such modifications change sieving behavior.
3. Use electron beam physical vapor deposition to coat SNM with a thin layer of silver.
4. Vary the voltage applied to a metallized SNM and measure how this voltage changes its associated apparent zetapotential via the streaming potential method.
5. Measure how varying the voltage applied to the conductive layer changes the sieving properties for charged gold nanoparticles and DNA undergoing electrophoresis (i.e. *construct a nanofluidic transistor*)

Specific Aim 2: Experimentally establish the parameters that determine SNM sieving behavior

- Perform experiments evaluating sieving behavior while modulating pore size and porosity, the intrinsic charge of the membrane, the size, charge, and shape of the solute(s), the ionic strength of the solvent, the type of membrane, and the pressure driving the separation.

Specific Aim 3: Develop a predictive model of the sieving characteristics of SNM

1. Develop a predictive analytic model of convective transport incorporating charge-charge interactions for the filtration of both proteins and gold nanoparticles.
2. Use our model to select the parameters to maximize the relevant sieving coefficients for separations of β2-Microglobulin and Albumin for application in human hemodialysis.

Significance

Practical microfluidics - in the form of inexpensive devices that manipulate fluid in channels with dimensions in the micrometer range - promises to transform sample analysis in the laboratory and the hospital. A host of novel components, including pumps [6], mixers [7], valves [8], and even low performance nanofluidic transistors [9] have been demonstrated. Soft lithography PDMS technology has allowed many of these to be rapidly and cheaply incorporated into devices [10]. Despite these achievements, the technology is far from ubiquitous, and is considered to be "in early adolescence" [11].

One of the reasons microfluidic devices occupy only a small niche in analysis is the difficulty of preparing a sample for detection. Biological samples are typically dilute and complex, and concentration and filtration operations on small volumes are difficult. Silicon nanomembranes are freestanding porous membranes as thin as 15 nm with narrow pore distributions tunable within the range of 5-100 nm [1]. They have already been used successfully as filters of gold nanoparticles [2], and proteins [4]. Commercial nanomembranes, such as polycarbonate or cellulose membranes, are typically on the order of 1μm thick, and are composed of long, tortuous pores that are polydisperse in size [12]. Ultrathin membranes with holes drilled sequentially using a focused ion beam exist [9], but the manufacture process is too involved to scale up. Track-etched (TE) membranes nearly as thin as SNM exist, but these require access to a synchrotron radiation source, and silicon-based TE membranes are difficult to manufacture in large quantities [13]. Scalably manufacturable, ultrathin, monodisperse in pore distributions, and with hydraulic permeabilities dramatically better than any other nanomembrane (Figure 1), SNM may ultimately prove to be an important component in a host of microfluidic devices. The electrostatic interaction of a charged membrane and a charged species in solution is complex [14, 15] and important to understanding the sieving behavior of the membrane [16] because of the nanometer scale of the pores. The creation of SNM with dynamically modifiable surface charge would allow experiments probing these electrostatic interactions. In addition, SNMs with variable surface charge could be modified to create a high-performance nanofluidic transistor, which would have application to sample concentration and high level sample processing [17].

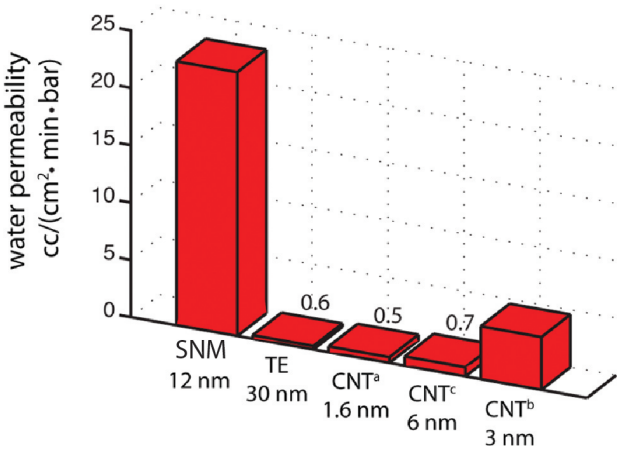

Figure 1: SNM have hydraulic permeabilities significantly better than both commercial track etched (TE) membranes and carbon nanotube membranes (CNT). (a) Holt *et al.* Science, 2006; (b) Yu *et al.* Nano Lett. 2009; (c) Majumder *et al.* Nature 2005. Image taken from [2]

Innovation

SNM have been metallized in the past for the creation of chemical capacitive sensing modules [18] and SNM have also had their surface charge chemically modified to change their sieving properties [5], but this proposal seeks to dynamically modify their surface charge via an insulated metal film on the membrane surface. This approach has been used previously on focused ion beam nanomembranes but those membranes had such limited active area that the wash required after a single switching event took two weeks [9] Since a typical SNM with 12% porosity has ~3 million times the open area

compared to focused ion beam membranes, we expect a substantial improvement (multiple orders of magnitude) in time response.

A model for the transport of small molecules through thin membranes due to diffusion does exist, but it ignores electrostatic interactions [3]. By identifying other relevant parameters and modifying surface charge, we will be afforded a unique window into the behavior of charged porous membranes.

Specific Aim 1: Modulate SNM pore sieving behavior via backfilling and active control of membrane surface charge

The objective of this aim is to precisely control the sieving properties of SNM by changing both the physical size of SNM pores and the electrostatic repulsion between the charged particles and the SNM due to membrane surface charge. By depositing oxide films on the surface of the membrane, we can modify the size of pores in the film. By depositing metal on the surface of the membrane and attaching an electrode to the film we can modify the surface charge of the membrane.

Aluminum oxide deposition via Atomic Layer Deposition (ALD) has already been demonstrated as an effective method of shrinking pores, and some preliminary data indicates that backfilled pores show decreased hydraulic permeability and decreased sieving coefficients for gold nanoparticles (Figure 2). Although pore size distributions can also be tuned by varying the temperatures and thermal ramp rates SNM wafers are subjected to during the manufacturing process [2], in practice it is difficult to target a particular average pore size, and a size ladder with the sufficient granularity needed to construct a model would be prohibitively costly (more than $17,000). ALD of aluminum oxide, on the other hand, is inexpensive (the URnano cleanroom in the basement of Goergen hall charges $12 for the half hour of machine time needed to run a batch, and a batch could reasonably include anywhere from individual chips to a full 6-inch silicon wafer of SNM with 394 chips). Also, because ALD is two-step and surface limited, film thickness can be controlled *to the angstrom* [19].

A nanoporous membrane composed of a bare gold film electrochemically deposited on a porous polycarbonate track-etched membrane has been demonstrated to vary ion sieving via an applied voltage in a three electrode setup [20], but the strong adsorption of Cl^- ions to Au [21] necessitates the use of unusual salts, such as KF, for device operation. Additionally, a bare gold film in solution would act as a nonpolarizing electrode (where the resistance between the electrode and the electrolyte $R \neq \infty$), which complicates the current flow in the device and makes modeling the performance of these membranes substantially more difficult [22]. For this reason, Paik et. al. used aluminum oxide (Al_2O_3, which has a resistivity of up to 10^{16} $\Omega\cdot$ cm for films thicker than 50 Å[23]) to insulate a metal film to allow the membrane surface charge to be dynamically modified [9]. Because the URnano cleanroom possesses a Lesker physical vapor deposition system (PVD 75) with the capacity to electron beam physical vapor deposit silver films with a precision of 1 nm, and because of in-house expertise regarding the deposition of silver films, we propose the creation of a membrane stack of a titanium adhesion layer, a silver film, and aluminum oxide as the final coating. Some optimization of conditions (Figure 3a) suggests that the stack in Figure 3b will give us an unbroken silver film insulated from bulk solution. ∼10 of these membranes were manufactured, and most of these had no obvious tears under a 20x objective in a microscope. The hydraulic permeability of one of the coated chips was tested and was comparable to other SNM with similar pore distributions. At that time we did not possess a working device for measuring the streaming potential of the membranes (see research design for more information), so it was not verified that a voltage applied to the membrane could modify the surface charge of the membrane.

Just as applying pressure across a charged membrane results in a voltage drop, applying a voltage results in a pressure drop. Our lab has exploited this phenomena to create electro-osmotic pumps using SNM [5]. Charged particles in the solution experience two competing forces: electrophoresis and

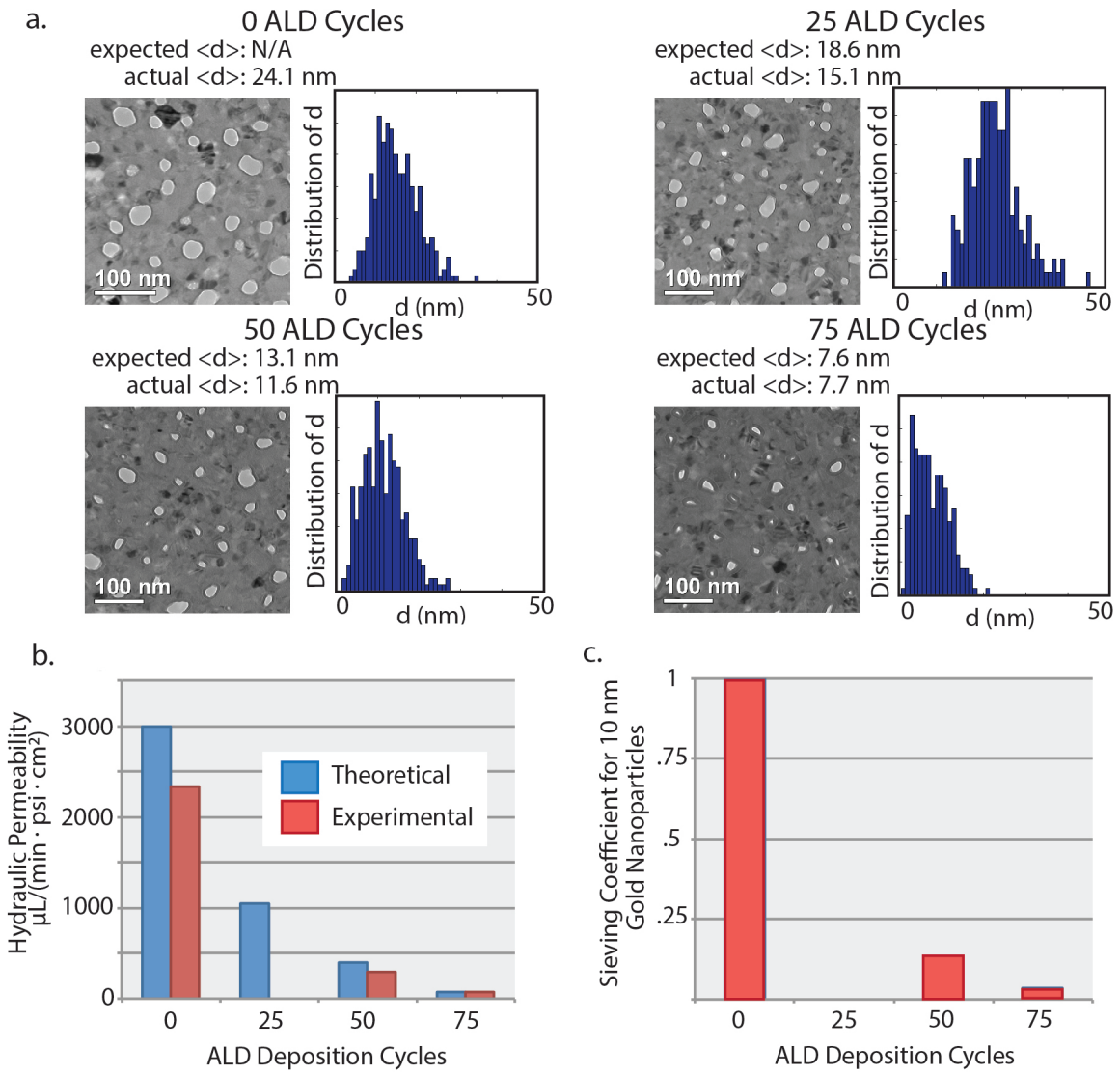

Figure 2: (a) TEM images show pores shrink after ALD deposition of aluminum oxide. (b) Plots of hydraulic permeabilities. Deviations from the theoretical permeabilities could result from either the difficulty inherent in measuring μL volumes (droplets tend to cling to surfaces) or else because of the non-circularity of the pores, which is not accounted for in our theoretical calculations (equation 5) (c) Sieving coefficients of gold show that sieving properties reflect the shrinking pore size. Note that the 25 ALD cycle chips broke before data could be collected for (b) and (c)

electro-osmosis. Since electro-osmosis arises from the charge on the membrane, a membrane with a variable charge can modulate the electro-osmotic force, and in this way electrically control the passage of charged species in a manner analogous to field effect transistors in solid state computation. These so-called nanofluidic transistors (NFT) represent a novel kind of sample processor, where the passage and capture of an analyte can be controlled through purely electrical means. NFT have been suggested for use as preconcentrators, especially in tandem with DNA sequencing techniques [9], as well as for advanced sample preparation in lab on a chip devices [24].

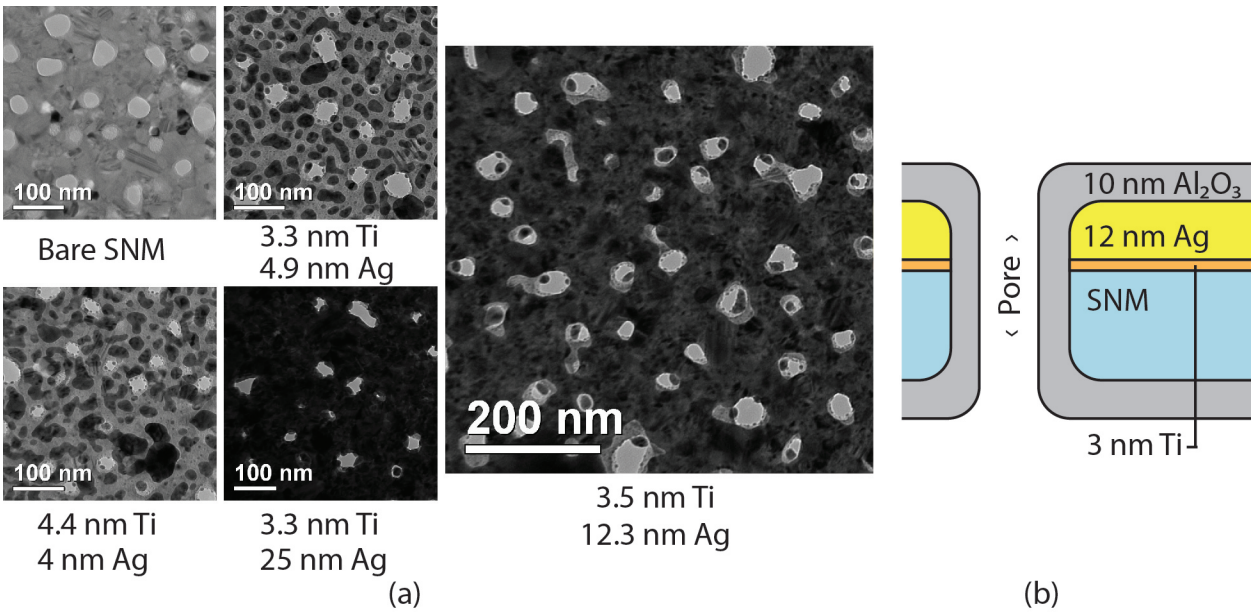

Figure 3: (a) A ladder of silver film thicknesses indicates 12 nm is sufficient thickness for an unbroken film. (b) The proposed film stack.

Research Design

Use Atomic Layer Deposition (ALD) to backfill SNM pores with Aluminum Oxide

The Cambridge Microsystems Savannah 200 atomic layer deposition system uses a two-step chemical process that alternates pulses of water vapor and trimethylaluminum (TMA) to build a layer of aluminum oxide on a silicon substrate [19]. Because of the two-step nature of the process, the film is forced to grow by successive monolayers, each with a thickness of 1.1 Angstroms (although this thickness is mildly temperature dependent) [19]. There is a library of standard recipes in the machine that allow for easy modification of the ultimate thickness of the aluminum oxide layer at both 200°C and 100°C. The manufacturing process for SNM includes a number of smaller chips with free standing membranes designed for insertion into a transmission electron microscope (TEM) in every wafer of SNM chips produced. These are used for characterizing pore distributions in either the URnano STEM or in the UR medical center Electron Microscope Research Core TEM. Hence, we include one or more of these TEM sized chips in the ALD chamber while SNM chips are being coated with aluminum oxide, enabling us to precisely monitor pore size distributions. Images taken with either the STEM or the TEM are analyzed using a custom Matlab (www.mathworks.com/products/matlab) program to generate pore size histograms, average pore size, and other representative statistics (Figure 4).

Demonstrate that modulating the pore size distribution and porosity of SNMs using ALD appropriately modifies sieving behavior

Gold nanoparticles, available from BBI solutions (BBIsolutions.com) in a size ladder from 5-200 nm, are excellent model particles for understanding the sieving properties of SNM. Gold nanoparticles absorb light because of surface plasmon resonance [25], and have such high optical density that they are visible in solution (at concentrations as low as 10 μM they turn the solution a coral pink). Commercial preparations are monodisperse in size. We use a Tecan infinite pro absorbance reader with a nanoquant plate that allows us to collect absorbance measurements with as little as 3 μL of analyte. Although the absorbance peak of gold is somewhat dependent on the size of the gold nanoparticles [25], we have

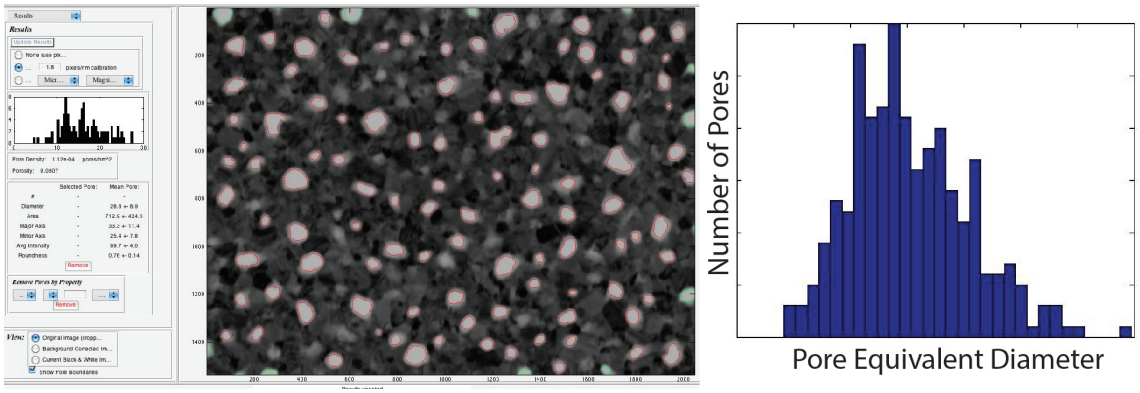

Figure 4: A custom Matlab program analyses a TEM image of a SNM and outputs a pore histogram and other statistics

found that absorbance at 515 nm is appropriate for calculating absorbance across a wide range of gold sizes. Concentration is determined by a standard curve, generated from a serial dilution of stock. A buffer signal is subtracted from each absorbance measurement. Gold nanoparticles have an inherent negative charge, which we have measured in our Malvern Zetasizer Nano as -30 mV for 10 nm gold. This charge is pH dependent [26] and is a result of the manufacturing process, which includes the addition of citric acid to the nascent gold particles [27]. This charge does complicate sieving behavior, and gold sieving has been shown to be sensitive to salt concentration [5]. An important consideration is that gold nanoparticles only tolerate a low salt concentration (they are somewhat unstable at 10 mM, and rapidly aggregate in 100 mM KCl). This is unfortunate because the debye length (L, the length over which charge-charge interactions are relevant) is dependent on salt concentration:

$$\text{Debye Length } L = \sqrt{\frac{\varepsilon_r \varepsilon_0 RT}{2F^2 C_0}} \text{ (for symmetric monovalent salts)} \tag{1}$$

where C_0 is ionic concentration, ε_0 is the permittivity of free space, ε_r is the dielectric constant of the solution, R is the gas constant, and F is Faraday's constant. This means that if gold nanoparticles were salt stable we could essentially eliminate electrostatic interactions with high salt concentrations. Uncharge colloids that do not aggregate exist [16], but these typically use steric exclusion to keep from aggregation, i.e. by coating a silica bead with a layer of a hydrophilic polymer [28].

For all experiments, SNM chips must be carefully assembled into a plastic housing that is sealed with silicone gaskets and pressurized using nitrogen gas in the system depicted in Figure 5.

Use E-Beam deposition to coat SNM with a thin layer of titanium, then silver

The Lesker physical vapor deposition system (PVD 75) uses an electron gun magnetically aimed at a metal ingot to heat the ingot and cause it to evaporate. Upon contacting a surface, the metal precipitates, initially as isolated islands, and then after further deposition as a uniform film covering everything in a line of sight from the source [29]. The chamber operates under high vacuum (5E-5 Torr), and deposition rates are controlled by adjusting the amperage applied to the electron gun, but are typically in the range of 1 Å/s to 1 nm/s. Because silver does not easily form an oxide it does not adhere well to the native oxide on the surface of the SNM [30]. To aid in adhesion, an adhesion layer composed of a transition metal with a low free energy of oxide formation, such as titanium, is used. Our previous results (Figure 3) suggest that 12 nm of silver is sufficient for an unbroken silver film.

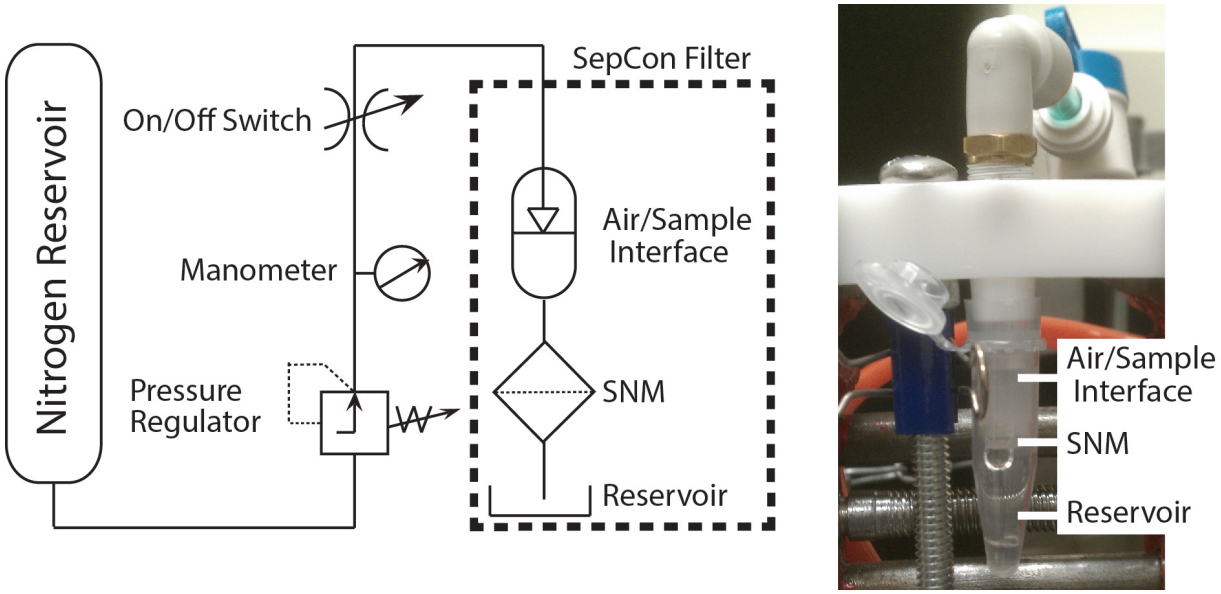

Figure 5: Schematic and picture of the experimental setup for filtration experiments. The system is driven using pressurized nitrogen gas, which is modulated by means of a pressure regulator and monitored with a manometer.

Verify that changing the voltage applied to a metallized SNM changes its associated apparent zeta potential via the streaming potential method

A streaming potential, or the voltage drop across a charged membrane when a salt solution is pumped across it, arises because a negatively charged membrane with sufficiently small pores preferentially allows cations to pass [5]. This phenomena can be exploited via the Helmholtz-Smoluchowski equation to give an apparent zeta potential:

$$\zeta = \frac{dE_z}{d\Delta P} \cdot \frac{\eta \Lambda}{\varepsilon_0 \varepsilon_r} \tag{2}$$

where ζ is the apparent zeta potential, E_z is the streaming potential, ΔP is the applied pressure, η is the solution viscosity, Λ is the solution conductivity, ε_0 is the permittivity of free space, and ε_r is the dielectric constant of the solution [26]. We based our streaming potential device on Burns et. al.'s device, but substantially modified it based on our particular needs [31] Our device is pictured in Figure 6. Note that the electrodes are easily replaced by removing the two associated nylon screws. This is important because the Ag/AgCl electrodes used degrade over time. This degradation happens because the Ag/AgCl electrodes are in rapid redox equilibrium with the KCl solution, and Cl^- ions enter or leave the electrode depending on the voltage applied [22]. The rapid redox equilibrium ensures that the electrodes can be approximated as ideal nonpolarizable electrodes and is the reason that Ag/AgCl electrodes are ubiquitous in microfluidics. Our electrodes are made by dipping small coils of silver wire into a commercial Ag/AgCl ink (agcl-675 silver/silver chloride, available from www.conductivecompounds.com). KCl is used for streaming potential measurements because of the similar mobilities of K^+ and Cl^- ions. Applied pressure is varied and monitored with a modified version of the pressure setup in Figure 5. Because this is a new design for the device, we will verify the surface charge measurements using conductance measurements [32]. Additionally, If hydraulic flow through the pores is significantly greater (or less) than that which would be predicted by the Dagan equation, it could be because the thin silver film is distort the TEM images we attain, resulting in larger (or smaller) pore distributions than are really in the silicon. Hence we will need to verify the pore distributions attained in the metallized SNM using hydraulic permeability data.

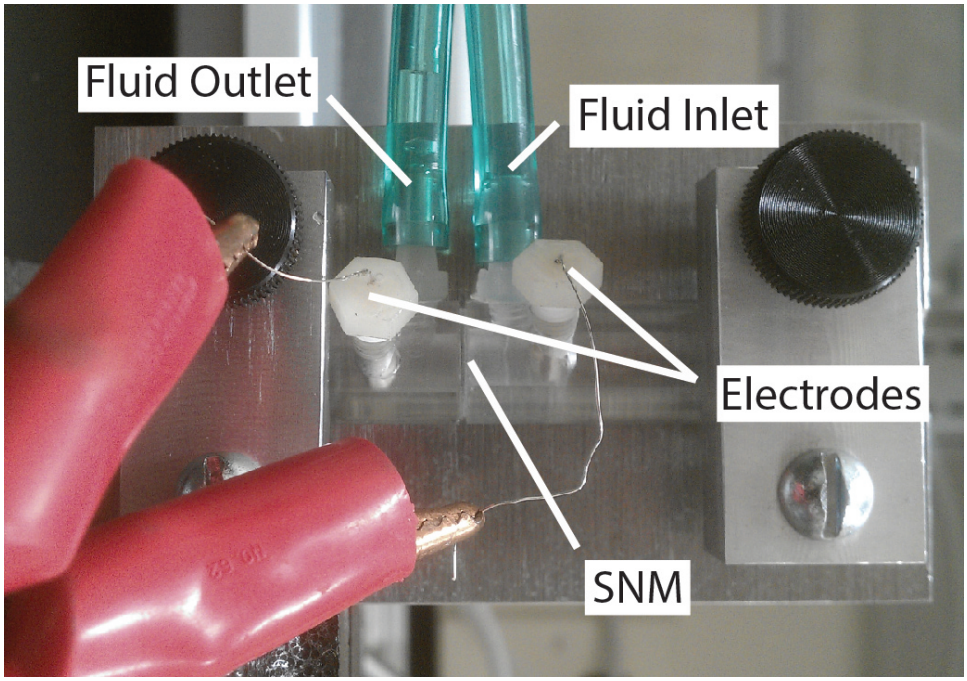

Figure 6: Experimental setup of streaming potential measurements. Water is pumped through the membrane via pressurized nitrogen gas, and the transmembrane voltage drop (the streaming potential) is measured across a range of applied pressures to obtain the apparent zetapotential.

Demonstrate that varying the voltage applied to the conductive layer can change the sieving properties for charged gold nanoparticles and DNA undergoing electrophoresis (i.e. construct a nanofluidic transistor)

Since there are already electrodes in the solution on both sides of the membrane, it will be trivial to hook the leads up to a function generator. If our membrane was totally uncharged, we would expect that charged species (e.g. DNA) would undergo electrophoresis and migrate towards the electrode with a charge opposite their own. Because we can adjust the membrane charge, we can gate the migration of these charged species. We will apply a voltage to the membrane such that it is strongly negatively charged. Negatively charged DNA and gold will be inserted into one side of the membrane, and a voltage difference will be established such that the charged species will be drawn towards the membrane, but will be unable to cross the membrane because of the overlapping double layers at the pore entrances. Periodic samples will be removed from the downstream chamber and analyzed to determine concentration of gold or DNA. Then the applied voltage on the membrane will change to be opposite that of the intrinsic charge on the membrane so that the total charge on the membrane is zero. Samples will be removed from the downstream chamber and compared to the samples when the membrane was negatively charged, and the effect that the gating voltage has on the flow of the charged species through the membrane will be established. Note that due to electro-osmotic flow we will expect to see a net flow of water through the membrane even if DNA or gold is held back, and our experimental setup will need to accommodate this hydraulic flux.

Aim 2: Experimentally establish the parameters that determine SNM sieving behavior

The factors governing the translocation of charged particles and proteins through a charged membrane are numerous, complex, and interrelated. Despite extensive investigation [33, 34, 31] many of the phenomena remain poorly understood. In the service of creating a predictive model (Aim 3) it is important to identify which factors are necessary to examine exhaustively and which can be ignored. Further, once relevant parameters are identified, experiments probing how changing said parameters influences sieving behavior and hydraulic permeability will give us an intuition for how each should be incorporated into the model, as well as provide experimental justification (or falsification) of any model we produce.

Studies in which a single variable, such as solution pH [35], ionic strength [36], pore size distribution [12], particle charge [16] etc. are changed and the effect upon sieving or permeability is measured and theoretically explained are common. However, the unique thinness of SNM means that these studies, which typically investigate membranes much thicker than SNM, may not apply to our novel material. In particular, many flow models [37] assume that the pores are infinitely long (Hagen-Poiseille flow) and pore entrance/exit effects can be ignored. But in SNM, which can contain pores with aspect ratios greater than 1, flow is not fully developed and entrance effects cannot be ignored.

Previously, the McGrath lab has investigated the influence of particle charge [16] and size [38] on the behavior of diffusive sieving across the membrane, and some experimental work has been done with gold and protein ladders in pressurized flow experiments [2]. Additionally, we have done some initial experiments demonstrating that changing applied pressure, system geometry (Figure 7), and pore size and porosity through ALD of aluminum oxide (Figure 2) can change the sieving behavior of the SNM.

Research Design

Perform experiments evaluating sieving behavior while modulating pore size and porosity, the intrinsic charge of the membrane, the size, charge, and shape of the solute(s), the ionic strength of the solvent, the type of membrane, and the pressure driving the separation.

Using the pressure cell depicted in Figure 5, variable KCl concentration, Bovine Serum Albumin (BSA) solutions, a size ladder of gold nanoparticles, and the ALD deposition process as experimental parameters, and a mass balance and Tecan absorbance machine(for quantification of hydraulic permeability and gold/protein concentration, respectively), we can expand our preliminary results into a reasonably complete experimental picture of sieving.

Porous nanocrystalline silicon (pnc-Si) is formed by rapidly thermally processing an amorphous silicon layer, then etching away oxide layers and bulk silicon to expose a freestanding membrane; such membranes typically break at applied pressures of between 8 and 10 psi. Our current pressure setup works best at pressures between 2 and 30 psi, so an appropriate pressure range would be 2-7 psi of applied nitrogen at intervals of 1 psi. Recently, our lab has developed a new SNM where a pnc-Si layer is used as a template for etching a silicon nitride layer. This new process may change the surface properties of the SNM, but the nitride membranes are substantially stronger (they break at applied pressures of 25-30 psi), so once we more fully understand the surface properties of silicon nitride membranes it is possible we may move away from pnc-Si. With silicon nitride an appropriate pressure range would be in the 2-25 psi range, with the caveat that at higher pressures our current pressure cell would need to be modified so that a greater volume of sample could be placed above the membrane. This is because at such high pressures the typical loading volume of the current pressure

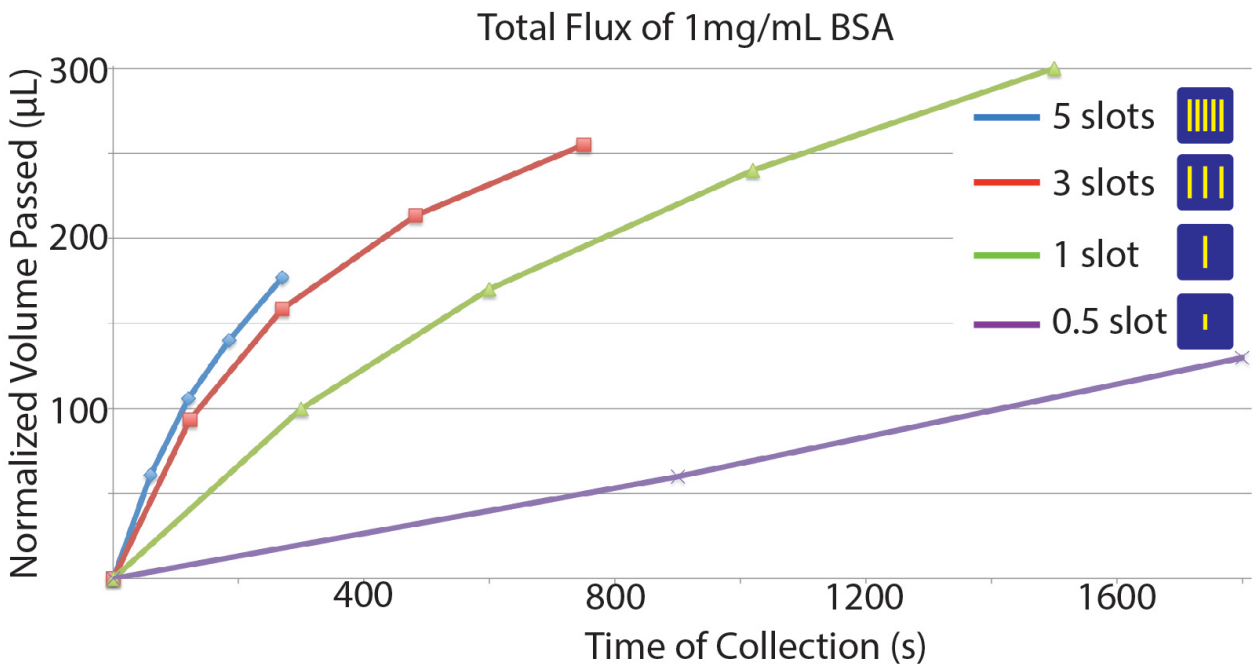

Figure 7: Flux (volume passed) of a protein solution through SNM depends on SNM geometry. Even when flux is normalized (half-slot chip flux is multiplied by 10 to compare it to the five slot chip, one slot flux by 5, etc.) SNM with a larger active area still show smaller time-dependent reductions in flux. This is likely due to an increase in concentration polarization in the chips with smaller active area, but as the pores have dimensions in the tens of nanometers and the geometry has dimensions on the order of millimeters, this phenomena requires further investigation.

setup (< 500 μL) would pass through the membrane too rapidly for a human operator to repeatably stop the system after a given amount of sample flux.

BBI (www.bbisolutions.com) sells gold nanoparticles in sizes up to 250 nm in diameter, but at sizes larger than 50 nm the particles begin settling quickly enough to interfere with an experiment (even 20 nm gold should be vortexed after sitting for more than a week or so). We will therefore use a size ladder of 5, 10, 15, 20, 30, 40, and 50 nm, which are all sizes that we currently own in sufficient quantities for experiments. All protein experiments will be done using freshly mixed Bovine Serum Albumin (Cal Biotech, fraction V, low heavy metals, powder form). Note that BSA is ellipsoidal, and as a result it's hydrodynamic radius is larger than would be expected for a similar, spherical protein with the same volume. Further, BSA has an isoelectric point of 5.4, but its charge, like the charge of all proteins, is not evenly distributed on its surface [39] . This will complicate sieving behavior, and is something we will need to consider for modeling.

KCl concentrations of 100 mM render gold colloids unstable, so we treat 10 mM as the upper bound for gold separations, and 0.5 M for the upper bound in BSA experiments [40]. In the past, we have had problems with KCl aggregates that were clogging the membranes and causing a significant time dependence in the hydraulic permeability, but we have found that filtering the mixed salt(99.9% pure KCl (powder), Sigma Aldrich) at the desired concentration through a 0.2μm filter (Pall acrodisc 32 mm syringe filter w/ 0.2 μm supor membrane) results in constant hydraulic permeabilities. KCl concentrations are also verified by measuring the conductance of the solution using an Oakion CON6 conductivity probe.

This parameter space is large (five adjustable parameters), and if we assume that each variable is interdependent in a complex way a full characterization of the separation behavior of the gold would require an impractical number of experiments. Instead, we treat each adjustable variable

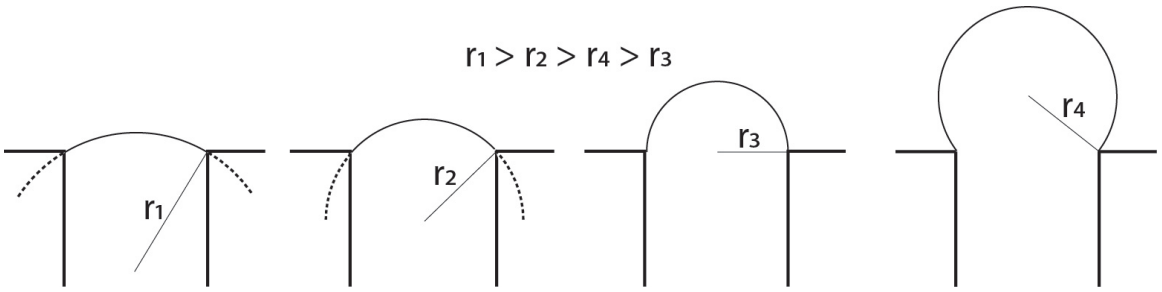

Figure 8: The radius of the sphere (r) that the meniscus in a narrow capillary tube would fit goes through a minimum when r = the pore diameter

(membrane charge, particle size, ionic strength of solution, applied pressure, and pore size distribution) as independent, and vary each one in isolation while holding the others constant. This is a simplistic view, since for instance solvent strength and the charge on the membrane are interdependent in determining sieving behavior, so as experimental results or our theoretical model indicated that a relationship between two variables needs closer examination we will then perform experiments with two adjustable parameters at once as needed. This compromise reduces the number of necessary experiments to a reasonable level.

Deionized water from a Barnstead nanopure diamond system is used for all preparations. A quirk of SNM is that the membrane must be manually wetted on both sides of the membrane in order for fluids to pass. The reason for this comes from the Young-Laplace equation (also called Laplace's equation):

$$\Delta P = \frac{2\gamma}{r} \tag{3}$$

where ΔP is the pressure applied to a narrow capillary tube, γ is the surface tension of the interface (0.07 N/m for air/water) and r is the radius of the sphere that the meniscus would fit. Note that as water is forced out the end of a capillary tube, r moves through a local minimum (when the contact angle is 90°, see Figure 8). For water to be forced through a 15 nm pore would require more than 2000 psi. For irregular pores, the droplet will not be perfectly spherical and the radius of the droplet will need to be represented by two radii of curvature, but such a correction is minor and cannot bring the critical pressure down the nearly two orders of magnitude necessary to cause backside wetting to occur at ¡ 8 psi. Wetting is accomplished manually by pipetting 12 μL of either water or the salt concentration being investigated onto the back of the membrane. This wetting aliquot must be included in concentration calculations.

The sieving coefficient is defined as $S \equiv \frac{C_{\text{feed}}}{C_{\text{filtrate}}}$, where C_{feed} and C_{filtrate} represent the solute concentration in the feed and filtrate solutions, respectively. The concentration of gold will be measured based on absorbance at 515 nm using a Tecan infinite pro absorbance reader as described in Aim 1. BSA quantification likewise will use absorbance at 280 nm.

Hydraulic permeabilities will be evaluated by solvent flux according to the formula

$$\text{Permeability} = \frac{V}{t \cdot \Delta P \cdot a} \tag{4}$$

where V is volume passed, t is collection time, and a is active area. Volume will be measured via weighing the filtrate. Because the volumes can be low, care must be taken that no droplet is hanging off of the bottom bucket. To this end, whenever a filtrate bucket is removed from the pressure assembly, the lip of the bucket is dragged across the bottom of the inner basket, ensuring that as much of the filtrate as possible is collected.

Specific Aim 3: Develop a predictive model of the sieving characteristics of SNM

Convective transport of proteins and small molecules through long tortuous pores as a combination of convection and diffusion has been thoroughly investigated from a hydrodynamic perspective for more than twenty years [41, 42], but most of these formulations take for their starting point a membrane composed of cylindrical or tortuous pores. Silicon nanomembranes are such a thin material that the transit time of a protein passing through the pore is almost negligible [2], which is not the case for other comparable membranes. Previously the McGrath lab has published both a Comsol finite element model and an analytic model that describes diffusion through molecularly thin membranes such as SNM [3] but it has not yet been extended to the convective regime. Additionally, no model exists for the behavior of SNM during the filtration of protein solutions. Protein adsorption to membrane surfaces is a ubiquitous problem in separation experiments, and has been well characterized [43]. Our hypothesis is that the membrane is so thin that diffusion, which is typically irrelevant in thicker membranes, will contribute enough to the transport of proteins to help offset the local concentration increase at the mouth of the pore (termed concentration polarization) that leads to protein adsorption, leading to substantially improved long-term performance.

Research Design

Develop a predictive model of convective transport incorporating charge-charge interactions for the filtration of both proteins and gold nanoparticles using a numerical solution to an analytic description of convective transport.

We have constructed an initial Matlab model that follows the process flow indicated in Figure 9 to obtain sieving coefficients for charged gold nanoparticles.

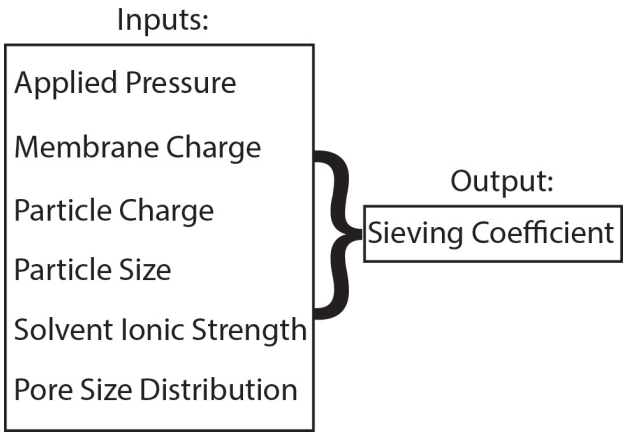

Figure 9: Inputs and Output of our Matlab model

Filtrate concentration of gold can be understood as the ratio of solvent (water) flux to solute (gold) flux through the membrane. Solvent flux can be found from the applied pressure using the Dagan Equation:

$$Q = \frac{\Delta P r^3}{\mu \left[3 + \frac{8}{\pi}\left(\frac{l}{r}\right)\right]} \tag{5}$$

(where Q, μ, r, and l are the solvent flux, solvent viscosity, pore radius, and pore length, respectively) which is an extension of the Hagen-poiseille equation to pores that cannot be approximated as infinitely long [44]. Solutes at least a few times bigger than the solvent molecules (gold can be as small as 5 nm diameter; a water molecule is ∼0.25 nm long) can be treated as Brownian particles subject to hydrodynamic resistance. For simple diffusion (i.e. spherical particles in an unbounded fluid) the solute flux is given by Fick's Law of Diffusion as $N_s = -D_\infty \frac{dC}{dz}$, where D_∞ is the diffusivity of a solute molecule as given by the Stokes-Einstein equation, C is concentration, and z is distance from the pore. Because of steric and electrostatic interactions, the free diffusion of particles is 'hindered' within the narrow confines of the pore, so that the diffusive term is actually $N_s = -K^{-1} D_\infty \frac{dC}{dz}$, with a diffusive hindrance factor (also called the enhanced drag) K^{-1}. Similarly, purely convective transport can characterized by $N_s = GVC$, with V representing the bulk flow and G the convective hindrance factor (also called the lag coefficient). Solute flux is a sum of the diffusive

and convective components of flux through the membrane:

$$\text{Solute Flux } = N = -K^{-1}D_{\infty}\frac{dC}{dz} + GVC \tag{6}$$

[42] Deen derived the following system of equations to describe solute flux N:

$$Pe = \frac{W\langle V\rangle L}{HD_{\infty}} \tag{7}$$

$$H = 2\int_0^{1-\alpha} K^{-1}e^{-E(\beta)/kT}\beta d\beta \tag{8}$$

$$W = 4\int_0^{1-\alpha} G(1-\beta^2)e^{-E(\beta)/kT}\beta d\beta \tag{9}$$

$$\langle N\rangle = W\langle V\rangle C_{\text{feed}}\frac{[1-(C_{\text{filtrate}}/C_{\text{feed}})e^{-Pe}]}{1-e^{-Pe}} \tag{10}$$

[42] where $\beta = \frac{r}{\text{pore radius}}$ is the dimensionless radial position, Pe is the Peclet number (the ratio of convective to diffusive transport in the system), $\alpha = \frac{\text{particle radius}}{\text{pore radius}}$, and $E(\beta)$ is the boltzman energy. Note that the last equation can be re-written so that C_{filtrate} (which is what we are solving for) can drop out. H and W are two hydrodynamic functions that modify the diffusive and convective flux (respectively) due to steric and electrostatic interactions. Note that the limiting cases for equation 10 are $\langle N\rangle = W\langle V\rangle C_{\text{feed}}$ for $Pe >> 1$ and $\langle N\rangle = \frac{HD_{\infty}}{L}(C_{\text{feed}} - C_{\text{filtrate}})$ for $Pe << 1$. K^{-1} and G are interpolated from Paine and Scherr's [45] numerical simulations using a polynomial fit of their data of order 40. It's important to note that Paine and Scheer assume that there is no electrostatic repulsion ($E(\beta) = 0$) within the pore for the calculation of these values. Dechadilok and Deen examine electrostatic effects on both G [46] and K^{-1} [38]; they found that accounting for electrostatics did marginally change both values, but the greater impact of charge-based repulsion came from whether or not the particles made it into the pore in the first place. Since we are accounting for electrostatics elsewhere, Paine and Sheer is a reasonable approximation. Note also that extensive experimental evidence indicates that the viscosity of water in pores down to a size of $30\mathring{A}$ does not deviate significantly from its bulk value [42], and we can thus treat viscosity as uniform everywhere in our system.

The final component we need to create a mathematical model of gold transport through the membrane is a formulation of $E(\beta)$. This is considerably more complicated than dealing with the neutral pore/neutral particle case. We intend to use the Smith and Deen model of solute partitioning within a charged pore, which uses the linearized Poisson-Boltzman equation in both spherical and cylindrical coordinates to find an expression for the change in free energy between a charged particle in the bulk ionic solution and a charged particle within the confines of a charged pore [47] (see Appendix for a further discussion of the Smith and Deen model). This will be implemented in Matlab and solved numerically. We will continue to add to and modify the model using feedback from the experiments in Aim 2 in an iterative process. The criterion for success of this model will be when the model can predict the expected sieving coefficient of gold nanoparticles over the range of pressures, gold sizes, and porosities investigated in Aim 2 to within experimental error, as in the Snyder et. al. model for diffusion of small molecules [3]. Then we will expand the model using the Ho and Zydney model of cake layer filtration, which characterizes the time-dependent flux behavior of microfiltration membranes as protein first blocks pores, then forms a cake layer over the membrane [43].

Use our model to select the parameters to maximize the relevant sieving coefficients for separations of β2-Microglobulin and Albumin for application in human hemodialysis

A suitable test for our model would be the optimization of a separation necessary for human hemodialysis. Current hemodialysis membranes are expensive, and are poor at imitating the cutoffs the human kidney is capable of (Figure 10a)

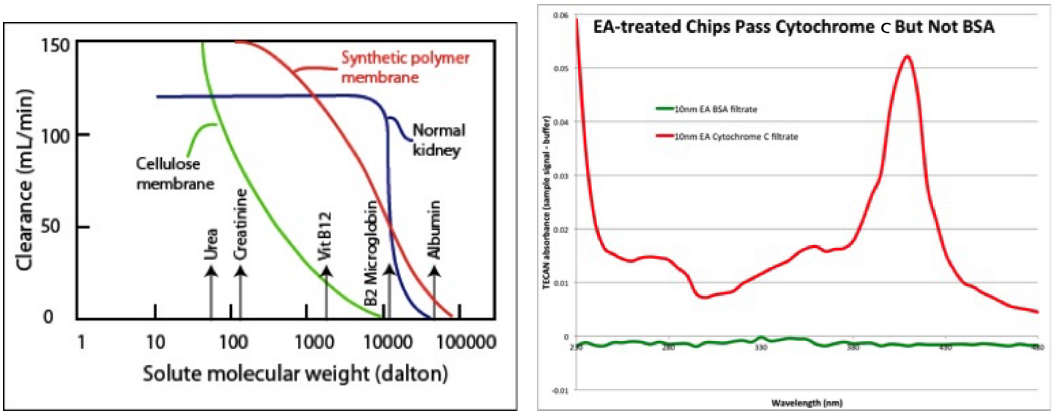

(a) (b)

Figure 10: (a)Typical dialysis membranes do a poor job of fractionating the components of blood. Note that the cellulose membranes pictured retain both β2 - Microglobulin and albumin, while the synthetic polymer membrane removes both β2 - Microglobulin and albumin, so that neither process is ideal. Image adapted from Advanced Membrane Technology and Applications; Norman N Li (Editor), Anthony G. Fane (Editor), W. S. Winston Ho (Editor), Takeshi Matsuura (Editor) (b) SNM with a pore cutoff of 10nm treated with a polymer coating are able to pass Cytochrome c (a molecule similar in size to β2 - Microglobulin, a toxin that must be removed as part of hemodialysis) but not BSA (albumin must be retained in any blood being dialysed) as measured by light absorbance. Note that Cytochrome c and BSA have very different absorbance spectra, so the two absorbance curves are not directly comparable. When compared to their respective standard curves, 12% of Cytochrome c passed through the membrane, while only 3% of BSA did. This separation indicates that the membrane would be useful for hemodialysis.

Additionally, dialysis represents a huge loss of mobility on the part of the patient, as typical dialysis treatments last for several hours several times a week. Our lab is working on the construction of a wearable, portable dialysis machine that uses SNM for separations.

Cytochrome c is not present in human blood, but it is a molecule analogous to β2 - Microglobulin, which is a toxin that any artificial kidney would need to remove (while retaining albumin). BSA is an inexpensive molecule similar to human albumin. We have already shown that SNM are capable of resolving Cytochrome c and BSA (Figure 10b). Using our model, we will find the maximum sieving coefficient (concentration of albumin/concentration of β2 - Microglobulin) given the experimental variables outlined in Figure 9.

References

[1] Christopher C Striemer, Thomas R Gaborski, James L McGrath, and Philippe M Fauchet. Charge-and size-based separation of macromolecules using ultrathin silicon membranes. *Nature*, 445(7129):749–753, 2007.

[2] Thomas R. Gaborski, Jessica L. Snyder, Christopher C. Striemer, David Z. Fang, Michael Hoffman, Philippe M. Fauchet, and James L. McGrath. High-performance separation of nanoparticles with ultrathin porous nanocrystalline silicon membranes. *ACS Nano*, 4(11):6973–6981, 2010.

[3] J.L. Snyder, A. Clark Jr., D.Z. Fang, T.R. Gaborski, C.C. Striemer, P.M. Fauchet, and J.L. McGrath. An experimental and theoretical analysis of molecular separations by diffusion through ultrathin nanoporous membranes. *Journal of Membrane Science*, 369(1–2):119 – 129, 2011.

[4] Dean G. Johnson, Tejas S. Khire, Jon-Paul S. DesOrmeaux, Tom R. Gaborski, Jeremy Taylor, Chris C. Striemer, and James L. McGrath. Ultrathin silicon membranes for wearable dialysis. *Advances in Chronic Kidney Disease (in press)*.

[5] J.L. Snyder, D.Z. Fang, T.R. Gaborski, C.C. Striemer, P.M. Fauchet, and J.L. McGrath. High performance, low voltage electroosmotic pumps with molecularly thin nanoporous membranes. *Proc. Natl. Acad. Sci. - submitted*, 2013.

[6] DJ Laser and JG Santiago. A review of micropumps. *Journal of micromechanics and microengineering*, 14(6):R35, 2004.

[7] Nam-Trung Nguyen and Zhigang Wu. Micromixers: a review. *Journal of Micromechanics and Microengineering*, 15(2):R1, 2005.

[8] Jong Wook Hong and Stephen R Quake. Integrated nanoliter systems. *Nature biotechnology*, 21(10):1179–1183, 2003.

[9] Kee-Hyun Paik, Yang Liu, Vincent Tabard-Cossa, Matthew J. Waugh, David E. Huber, J Provine, Roger T. Howe, Robert W. Dutton, and Ronald W. Davis. Control of dna capture by nanofluidic transistors. *ACS Nano*, 6(8):6767–6775, 2012.

[10] J. Cooper McDonald, David C. Duffy, Janelle R. Anderson, Daniel T. Chiu, Hongkai Wu, Olivier J. A. Schueller, and George M. Whitesides. Fabrication of microfluidic systems in poly(dimethylsiloxane). *ELECTROPHORESIS*, 21(1):27–40, 2000.

[11] George M Whitesides. The origins and the future of microfluidics. *Nature*, 442(7101):368–373, 2006.

[12] Seiichi Mochizuki and Andrew L. Zydney. Theoretical analysis of pore size distribution effects on membrane transport. *Journal of Membrane Science*, 82(3):211 – 227, 1993.

[13] W.M. Zhang, J. Li, L.X. Cao, Y.G. Wang, W. Guo, K.X. Liu, and J.M. Xue. Fabrication of nanoporous silicon dioxide/silicon nitride membranes using etched ion track technique. *Nuclear Instruments and Methods in Physics Research Section B: Beam Interactions with Materials and Atoms*, 266(12–13):3166 – 3169, 2008. ¡ce:title¿Radiation Effects in Insulators¡/ce:title¿ ¡ce:subtitle¿Proceedings of the Fourteenth International Conference on Radiation Effects in Insulators¡/ce:subtitle¿ ¡xocs:full-name¿Fourteenth International Conference on Radiation Effects in Insulators¡/xocs:full-name¿.

[14] Cunlu Zhao and Chun Yang. Advances in electrokinetics and their applications in micro/nano fluidics. *Microfluidics and Nanofluidics*, 13(2):179–203, 2012.

[15] X.L. Wang, Y.Y. Fang, C.H. Tu, and B. Van der Bruggen. Modelling of the separation performance and electrokinetic properties of nanofiltration membranes. *International Reviews in Physical Chemistry*, 31(1):111–130, 2012.

[16] J.L. Snyder, P.J. Black, D.Z. Fang, T.G. Gaborski, C.C. Striemer, W.A. Bernhard, P.M. Fauchet, and J.L. McGrath. Electrostatic interactions and physicochemical characteristics of diffusing species influence separations with charged ultrathin membranes. *pnas (in review)*.

[17] Salvador Mafe, José A. Manzanares, and Patricio Ramirez. Gating of nanopores: Modeling and implementation of logic gates. *The Journal of Physical Chemistry C*, 114(49):21287–21290, 2010.

[18] Maryna N. Kavalenka, Christopher C. Striemer, Jon-Paul S. DesOrmeaux, James L. McGrath, and Philippe M. Fauchet. Chemical capacitive sensing using ultrathin flexible nanoporous electrodes. *Sensors and Actuators B: Chemical*, 162(1):22 – 26, 2012.

[19] Steven M. George. Atomic layer deposition: An overview. *Chemical Reviews*, 110(1):111–131, 2010. PMID: 19947596.

[20] C. R. Martin, M. Nishizawa, K. Jirage, M. Kang, and S. B. Lee. Controlling ion-transport selectivity in gold nanotubule membranes. *Advanced Materials*, 13(18):1351–1362, 2001.

[21] S. Biggs, P. Mulvaney, C. F. Zukoski, and F. Grieser. Study of anion adsorption at the gold-aqueous solution interface by atomic force microscopy. *Journal of the American Chemical Society*, 116(20):9150–9157, 1994.

[22] Tim Albrecht. How to understand and interpret current flow in nanopore/electrode devices. *ACS Nano*, 5(8):6714–6725, 2011.

[23] M.D. Groner, J.W. Elam, F.H. Fabreguette, and S.M. George. Electrical characterization of thin al2o3 films grown by atomic layer deposition on silicon and various metal substrates. *Thin Solid Films*, 413(1–2):186 – 197, 2002.

[24] Xiaozhong Jin and N.R. Aluru. Gated transport in nanofluidic devices. *Microfluidics and Nanofluidics*, 11(3):297–306, 2011.

[25] Wolfgang Haiss, Nguyen T. K. Thanh, Jenny Aveyard, and David G. Fernig. Determination of size and concentration of gold nanoparticles from uvvis spectra. *Analytical Chemistry*, 79(11):4215–4221, 2007. PMID: 17458937.

[26] R.J. Hunter. *Zeta Potential in Colloid Science: Principles and Applications*. Colloid science. Academic Press, 1988.

[27] Wolfgang Haiss, Nguyen T. K. Thanh, Jenny Aveyard, and David G. Fernig. Determination of size and concentration of gold nanoparticles from uvvis spectra. *Analytical Chemistry*, 79(11):4215–4221, 2007. PMID: 17458937.

[28] Jinhyang Choi, Andrew A. Burns, Rebecca M. Williams, Zongxiang Zhou, Warren R. Zipfel, Ulrich Wiesner, Alexander Y. Nikitin, and Andrea Flesken-Nikitin. Core-shell silica nanoparticles as fluorescent labels for nanomedicine. *Journal of Biomedical Optics*, 12(6):064007–064007–11, 2007.

[29] P.K.S.K.S.S. Harsha. *Principles of Vapor Deposition of Thin Films*. Elsevier Science, 2005.

[30] K.W. Vogt, P.A. Kohl, W.B. Carter, R.A. Bell, and L.A. Bottomley. Characterization of thin titanium oxide adhesion layers on gold: resistivity, morphology, and composition. *Surface Science*, 301(1–3):203 – 213, 1994.

[31] Douglas B. Burns and Andrew L. Zydney. Buffer effects on the zeta potential of ultrafiltration membranes. *Journal of Membrane Science*, 172(1–2):39 – 48, 2000.

[32] Ronald Kox, Stella Deheryan, Chang Chen, Nima Arjmandi, Liesbet Lagae, and Gustaaf Borghs. Local solid-state modification of nanopore surface charges. *Nanotechnology*, 21(33):335703, 2010.

[33] M. Napoli, J. C. T. Eijkel, and S. Pennathur. Nanofluidic technology for biomolecule applications: a critical review. *Lab Chip*, 10:957–985, 2010.

[34] Amy E. Childress and Menachem Elimelech. Relating nanofiltration membrane performance to membrane charge (electrokinetic) characteristics. *Environmental Science and Technology*, 34(17):3710–3716, 2000.

[35] Meisam Bakhshayeshi and Andrew L. Zydney. Effect of solution ph on protein transmission and membrane capacity during virus filtration. *Biotechnology and Bioengineering*, 100(1):108–117, 2008.

[36] Raymond H. C. M. van Eijndhoven, Skand Saksena, and Andrew L. Zydney. Protein fractionation using electrostatic interactions in membranel filtration. *Biotechnology and Bioengineering*, 48(4):406–414, 1995.

[37] Panadda Dechadilok and William M. Deen. Hindrance factors for diffusion and convection in pores. *Industrial and Engineering Chemistry Research*, 45(21):6953–6959, 2006.

[38] Panadda Dechadilok and William M. Deen. Electrostatic and electrokinetic effects on hindered diffusion in pores. *Journal of Membrane Science*, 336(1–2):7 – 16, 2009.

[39] Putman FW, editor. *The Plasma Proteins*. Academic Press, 1975.

[40] Jonathan Rubin, Adriana San Miguel, Andreas S. Bommarius, and Sven H. Behrens. Correlating aggregation kinetics and stationary diffusion in proteinsodium salt systems observed with dynamic light scattering. *The Journal of Physical Chemistry B*, 114(12):4383–4387, 2010. PMID: 20178329.

[41] John L. Anderson and John A. Quinn. Restricted transport in small pores: A model for steric exclusion and hindered particle motion. *Biophysical Journal*, 14(2):130 – 150, 1974.

[42] W. M. Deen. Hindered transport of large molecules in liquid-filled pores. *AIChE Journal*, 33(9):1409–1425, 1987.

[43] Chia-Chi Ho and Andrew L. Zydney. A combined pore blockage and cake filtration model for protein fouling during microfiltration. *Journal of Colloid and Interface Science*, 232(2):389 – 399, 2000.

[44] Zeev Dagan, Sheldon Weinbaum, and Robert Pfeffer. An infinite-series solution for the creeping motion through an orifice of finite length. *Journal of Fluid Mechanics*, 115:505–523, 2 1982.

[45] P.L. Paine and P. Scherr. Drag coefficients for the movement of rigid spheres through liquid-filled cylindrical pores. *Biophysical Journal*, 15(10):1087 – 1091, 1975.

[46] Panadda Dechadilok and William M. Deen. Electrostatic and electrokinetic effects on hindered convection in pores. *Journal of Colloid and Interface Science*, 338(1):135 – 144, 2009.

[47] Frank G Smith III and William M Deen. Electrostatic effects on the partitioning of spherical colloids between dilute bulk solution and cylindrical pores. *Journal of Colloid and Interface Science*, 91(2):571 – 590, 1983.

Appendix: Calculating ΔG

In Electrostatic Effects on the Partitioning of Spherical Colloids between Dilute Bulk Solution and Cylindrical Pores, Smith et. al. find

$$E(\beta) = R_0 \epsilon (RT/F)^2 \Delta G \tag{11}$$

where $R_0, \epsilon, R, F, \Delta G$ are the Cylinder radius, the solvent dielectric permittivity, the gas constant, the faraday constant, and the Gibbs free energy, respectively. ΔG at constant surface charge represents the change in free energy between a charged particle in solution and the charged particle within a charged pore, and is given as the following equation:

$$\Delta G = \frac{\frac{8\pi\tau\alpha^4 e^{\tau\alpha}}{1+\tau\alpha^2}\Lambda\sigma_s^2 + \frac{4\pi^2\alpha^2 I_0(\tau\beta)}{(1+\tau\alpha)I_1(\tau)}\sigma_s\sigma_c + \left(\frac{\pi I_0(\tau\beta)}{\tau I_1(\tau)}\right)^2 \frac{(e^{\tau\alpha}-e^{-\tau\alpha})\tau\alpha L(\tau\alpha))}{1+\tau\alpha}\sigma_c^2}{\pi\tau e^{-\tau\alpha} - \frac{2(e^{\tau\alpha}-e^{-\tau\alpha})\tau\alpha L(\tau\alpha)\Lambda))}{1+\tau\alpha}} \tag{12}$$

where τ is the ratio of pore radius to debye length (equation 1), $L(\tau\alpha) = \coth(\tau\alpha) - \frac{1}{\tau\alpha}$, I is the modified bessel function of the first kind, σ_s and σ_c are the surface charge of the sphere and the cylinder, respectively, and when the dielectric constant of the metal is much higher than that of the solvent, Λ can be approximated:

$$\Lambda \approx \frac{\pi}{2} I_0(\tau\beta) \sum_{t=0}^{\infty} \frac{\beta^t (2t)!}{2^3 (t!)^2} I_t(\tau\beta) \times \left[\tau K_{t+1}(2\tau) + \frac{3}{4} K_t(2\tau)\right] \tag{13}$$

where K is the modified bessel function of the second kind [47]. Note that σ_s and σ_c are both exclusively in the numerator of equation 12, meaning as either surface's charge increase the associated change in free energy likewise increases. Further note that because the surface charges are additive, even if one of the surfaces charges were zero there would still be an electrostatic component to the difference in free energy. Only if both of the particles had zero surface charge would this expression go to zero. This expression is derived by describing a charged sphere and a charged cylinder using the linearized Poisson-Boltzman equation in both spherical and cylindrical coordinates (respectively), identifying the boundary conditions of the two systems of equations, and then performing a coordinate transformation to apply one set of boundary conditions to the next.